UDC 533.9.01; 533.9…1
IRSTI 29.27.03; 29.27.47

https://doi.org/10.55452/1998-6688-2025-22-4-354-364

[1,2,3]*Ismagambetova T.N.,
PhD, Senior Lector, ORCID ID: 0000-0003-4889-7526,
*e-mail: ismagambetova@physics.kz
[1,2,4]Muratov M.M.,
PhD, Associate Professor, ORCID ID: 0000-0001-7270-9834,
e-mail: mukhit.muratov@gmail.com
[5]Ussenov Y.A.,
PhD, Associate Research Physicist, ORCID ID: 0000-0001-7903-8674,
e-mail: yussenov@pppl.gov
[2,3,4]Gabdullin M.T.
PhD, Cand.Phys.-Math.Sc., Professor, ORCID ID: 0000-0003-4853-3642,
e-mail: gabdullin@physics.kz

[1]National Nanotechnology Laboratory of Open Type (NNLOT),
Al-Farabi Kazakh National University, Almaty, Kazakhstan
[2]Institute of Applied Sciences and IT, Almaty, Kazakhstan
[3]Kazakh British Technical University, Almaty, Kazakhstan
[4]Kazakh Physical Society, Almaty, Kazakhstan
[5]Princeton Plasma Physics Laboratory, Princeton, NJ, USA

EFFECT OF IONIC CORE ON THE PROPERTIES OF NON-ISOTHERMAL PLASMAS

Abstract

This study investigates the effects of ionic cores on non-isothermal plasmas using a novel ion-ion interaction potential that incorporates screening effects from both ion cores and exchange-correlation interactions. Our findings indicate that with increasing distance, the effective potential approaches a Yukawa-like screening potential, while at shorter distances, strong electron binding weakens screening. The different values of the cutoff radius $'cut$ and core edge steepness α significantly influence the potential behavior and radial distribution functions (RDFs). Higher coupling parameters (Γ_i) strengthen the electron-ion interactions, leading to deeper potential wells and more pronounced non-ideality corrections. Increasing Θ decreases the absolute values of non-ideality corrections, indicating fewer interactions in the system. A larger cutoff radius r_{cut} at a fixed parameter α also reduces corrections due to weaker screening effects. As Γ_i increases, non-ideality corrections grow, reflecting stronger coupling. The results show the importance of taking into account the ion core effects in dense non-isothermal plasma research.

Keywords: dense plasmas, ion core, non-isothermal plasmas, ion-ion interaction potential, radial distribution functions, thermodynamic properties.

Introduction

The dense plasmas, characterized by a significant mass difference between ions and electrons, show non-isothermal behavior, making theoretical modeling more complex due to the slower response of ions to perturbations [1]. To model interactions accurately, researchers use the generalized Poisson-Boltzmann equation and derive effective interaction potentials from dielectric response functions [2–9].

Charge screening plays a key role in such dense plasmas, forming a polarization cloud of electrons that surrounds ions, compensating for the Coulomb potential. Excluding core electrons can be modeled with an empty core electron-ion pseudo-potentials [10–11]. Recent studies show that

ionic cores affect electron-ion scattering transport and temperature relaxation with strongly bound electrons altering the effective charge of ions and impacting the plasma's structural and thermodynamic properties for novel screened electron-ion, and the novel screened interaction potential for ion-ion pair [12–16].

These results showed the importance of considering ionic core effects in understanding dense plasma properties. Therefore, in this study, we want to continue the previous research based on the novel ion-ion interaction potential by analyzing the impact of the ionic core effects in non-isothermal plasmas. In this potential, both the screening effects due to the ion cores and from the exchange-correlation on the structural and thermodynamic properties are taken into account.

The paper is organized as follows: in Section 2, we describe the method used to compute the radial distribution functions (RDFs) and non-ideality corrections to the thermodynamic properties (internal energy and equation of state). In Section 3, the results and discussion of these calculations are presented.

Materials and methods

Ion–Ion Interaction Potential

In work (p. 2), a novel ion-ion screened potential that takes into account the ion core effect using a pseudo-potential model with strongly bound electrons was introduced by numerically solving the following formula [16–17]:

$$\Phi_{ii}(r) = \frac{Z^2e^2}{r} + \int \frac{d^3k}{(2\pi)^3} |\widetilde{\varphi_{ei}}(k)|^2 \chi_e(k) e^{i\vec{k}\vec{r}}, \quad (1)$$

where as a micro potential $\varphi_{ei}(r)$ the potential with soft empty cores, proposed by Gericke et al. was used [18]:

$$\varphi_{ei}(r) = \frac{Ze^2}{r}\left[1 - exp\left(-\frac{r^\alpha}{r_{cut}^\alpha}\right)\right], \quad (2)$$

where the parameter α controls the core edge steepness ($\alpha = 2\ and\ 6$), and r_{cut} is the core's cutoff radius ($r_{cut} = 0.75$ Å $\simeq 1.42a_B$, where $a_B = \hbar^2/(m_e e^2)$ is the first Bohr radius) – for beryllium ion. Their values align with Kohn-Sham DFT (Density Functional Theory), which accurately describes dense plasmas in partial degeneracy, while other values can be used for various interaction regimes.

$\chi_e(k)$ is the static electron-density response function which we used with the parameter γ in the form from work that corrects for non-ideality in electronic screening due to static local field effects, equivalent to the local density approximation in DFT, accurately describing screening in the uniform electron gas (UEG) and modeling the exchange-correlation part of the electron free energy density, $f_{xc}(n, T_e)$ [19–21]. The importance and novelty of use in the interaction potential of parameter γ were explained in more detail in the work (p. 3) [16].

Therefore, we used the following form of the inverse screening length:

$$k_e^2 = \frac{k_{id}^2}{1 - k_{id}^2\gamma},\ k_{id}^2 = k_{TF}^2\theta^{\frac{1}{2}}I_{-\frac{1}{2}}(\eta)/2,\ \gamma = -\frac{k_F^3}{4\pi e^2}\frac{\partial^2 n f_{xc}(n,T_e)}{\partial n^2}, \quad (3)$$

where $I_{-1/2}$ is the Fermi integral of the order $-1/2$, $\eta = \mu/k_B T_e$ is the reduced chemical potential, $k_{TF}^2 = 3\omega_p^2/v_F$ is the Thomas-Fermi wavenumber (ω_p is the plasma frequency, v_F is the Fermi velocity).

The following dimensionless parameters were used for non-isothermal plasma ($T_e \neq T_i$): the ion coupling parameter $\Gamma_{ii} \leq 10$ ($\Gamma_{ii} = \frac{Z_i^2 e^2}{a k_B T_i}\left(\frac{n_i}{n_e}\right)^{1/3} = \Gamma_{ee} Z_i^{5/3}\left(\frac{T_e}{T_i}\right) = \Gamma_{ei} Z_i^{2/3}\sqrt{\frac{T_e}{T_i}}$), where

$T_{ee} = T_e, T_{ii} = T_i$ and $T_{ei} = \sqrt{T_e T_i}$ [22], the degeneracy parameter $\Theta = \frac{k_B T}{E_F}$, where E_F is the Fermi energy, the density parameter $r_s = \frac{a}{a_B}$, where $a = (3/(4\pi n)^{1/3}$ is the mean inter-electronic distance (Wigner-Seitz radius), $R = r/a_B$ is measured in units of the first Bohr radius a_B.

To analyze the impact of the ion core, the potential (1) was compared with another screened Coulomb potential, known as the Yukawa potential, taking into account the exchange-correlation effect as described in equation (3) but without the ion core effect, and therefore, it will be denoted as simply the screened potential:

$$\Phi_Y(r) = \frac{Ze^2}{r}\exp(-k_e r). \quad (4)$$

The radial distribution functions of ions

The influence of the ionic core on structural properties was analyzed through the integral Ornstein-Zernike equation [23]:

$$h(r) = c(r) + n\int c(r')h(|\vec{r} - \vec{r}'|)d\vec{r}', \quad (5)$$

in the hyper-netted chain (HNC) approximation:

$$g_{HNC}(r) = exp[-\beta\Phi(r) + h(r) - c(r)], \quad (6)$$

where $\beta = (k_B T)^{-1}$ and $\Phi(r)$ is the interaction potential, $h(r)$ and $c(r)$ are the total and direct correlation functions. The details about solving the equations (5–6) can be found in works [20, 24–25] (p. 14).

The radial distribution functions (RDFs) calculated in the HNC approximation use an effective screened ion-ion potential that accounts for the use of the electron polarization function but does not double-count ion screening. This is confirmed by comparison with MD results in work [26], where both methods obtain similar RDFs.

Thermodynamic properties

The internal energy and equation of state were obtained using potential (2) and RDFs (5–6) [27]:

$$E = E_{id} - \pi\sum_{\alpha=i,e} n_\alpha \sum_{\beta=i,e} n_\beta \int_0^\infty g^{\alpha\beta}(r)\varphi^{\alpha\beta}(r)\, r^2\, dr = E_{id} - \Delta E, \quad (7)$$

$$P = P_{id} - \frac{2}{3}\pi\sum_{\alpha=i,e} n_\alpha \sum_{\beta=i,e} n_\beta \int_0^\infty \frac{\partial\varphi_{\alpha\beta}(r)}{\partial r} g_{\alpha\beta}(r)\, r^3\, dr = P_{id} - \Delta P, \quad (8)$$

where N is the number of particles in the system, $E_{id} = 3/2Nk_BT$ is the internal energy of an ideal plasma, $P_{id} = nk_BT$ is the equation of state of an ideal plasma, and $\varphi(r)$ is the micropotential used as the basis of the considered screened interaction potential.

Results and discussion

The screened interaction potential for ion–ion pair for non-isothermal plasma, calculated using Equation (1), based on the potential (2) to account for the ionic core and the density response function of the UEG for plasma electron screening.

Figures 1 and 2 show the interaction potentials for i-i pairs at $r_s = 1$. In Figure 1 the results for potential (1) at $\theta = 1$ and $\Gamma_i = 5$ are presented: the black solid line represents α=2 with $r_{cut} = 0.75$,

while the black dashed line corresponds to α=6 with the same r_{cut}. Additionally, the red solid line indicates α =2 with $r_{cut} = 0.25$, and the red dashed line represents α=6 for the same r_{cut}. The blue solid line shows the results for the screening potential (4).

In Figure 2 the interaction potentials (1) are displayed with various parameters. The black solid line (α =2) and dashed line (α =6) represent $\theta = 1, \Gamma_i = 1$, and $r_{cut} = 0.25$. The red solid and dashed lines correspond to $\theta = 1, \Gamma_i = 5$, both with $r_{cut} = 0.25$. Similarly, the green solid and dashed lines show $\theta = 1, \Gamma_i = 10$, also with $r_{cut} = 0.25$. Finally, the dotted lines represent the results for $\theta = 0.5$, α =2, and $r_{cut} = 0.25$, with black indicating $\Gamma_i = 1$, red for $\Gamma_i = 5$, and green for $\Gamma_i = 10$.

Figures 1 and 2 show that with increasing distance, potential (1) tends to the screening potential (4) (Yukawa), while at smaller distances, the strongly bound electrons shield the ion core, weakening the screening compared to the Yukawa potential. Increasing the r_{cut} at a fixed value of α leads to a softer potential (1), while decreasing α at a fixed r_{cut} results in a steeper potential (1) at short distances.

Higher Γ values indicate stronger coupling and deeper potential wells, meaning electron-ion interactions in the micro potential used as the basis become more significant as the system deviates from ideal gas behavior.

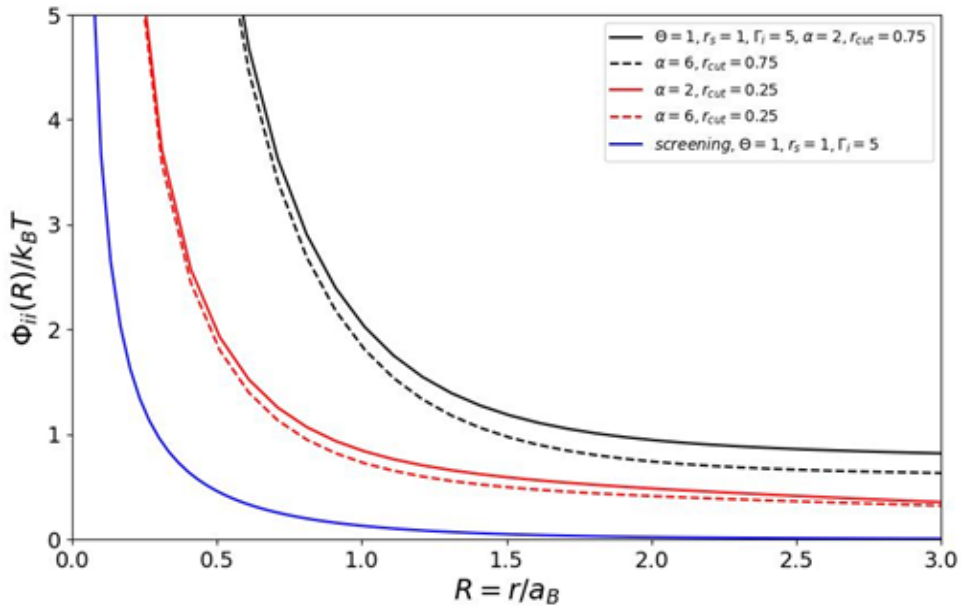

Figure 1 – The interaction potentials for i-i pairs at $r_s = 1$ for potential (1) $\theta = 1, \Gamma_i = 5$,
black solid line – α=2, $r_{cut} = 0.75$, black dashed line – α=6, $r_{cut} = 0.75$,
red solid line – α=2, $r_{cut} = 0.25$, red dashed line – α=6, $r_{cut} = 0.25$,
blue solid line – for screening potential (4)

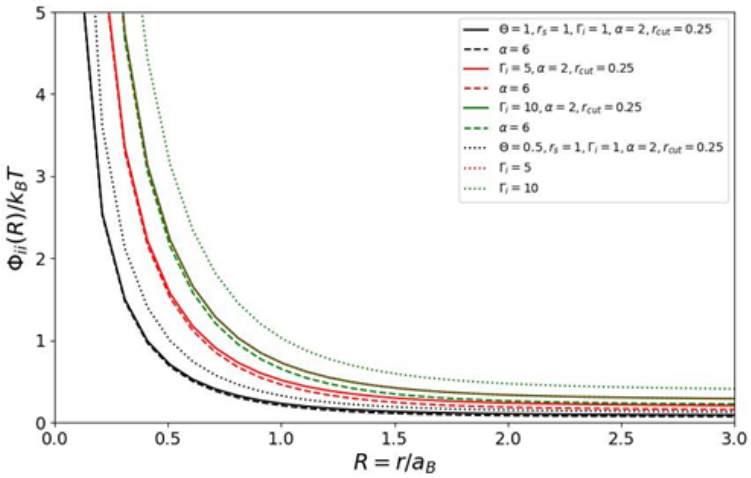

Figure 2 – The interaction potentials for i-i pairs at $r_s = 1$ for potential (1) black solid (α=2) and dashed (α=6) line – $\theta = 1, \Gamma_i = 1, r_{cut} = 0.25$, red solid ($\alpha$=2) and dashed ($\alpha$=6) line – $\theta = 1, \Gamma_i = 5, r_{cut} = 0.25$, green solid ($\alpha$=2) and dashed ($\alpha$=6) line – $\theta = 1, \Gamma_i = 10, r_{cut} = 0.25$, dotted lines represent results for $\theta = 0.5$, α=2, $r_{cut} = 0.25$ – black ($\Gamma_i = 1$), red ($\Gamma_i = 5$), green ($\Gamma_i = 10$)

Figure 3 shows the interaction potentials for ion-ion (i-i) pairs at a degeneracy parameter $\theta = 0.5$ and a density parameter $r_s = 1$, with $\alpha = 2$ for potential (1). The interaction potentials are plotted for various ratios of electron temperature to ion temperature (T_e/T_i). Specifically, the black solid line represents $T_e/T_i = 1$ with a cut-off radius $r_{cut} = 0.25$, while the black dashed line corresponds to $r_{cut} = 0.75$. The red lines depict $T_e/T_i = 2$, with the solid line for $r_{cut} = 0.25$ and the dashed line for $r_{cut} = 0.75$. Similarly, the blue lines represent $T_e/T_i = 3$, with the solid line again for $r_{cut} = 0.25$ and the dashed line for $r_{cut} = 0.75$.

As the ion temperature T_i decreases, the screening in the potentials increases. This increase is larger for a larger cut-off radius of $r_{cut} = 0.75$ at a constant $\alpha = 2$. This behavior is attributed to a strengthening in the attraction between bound electrons and ions. In contrast, as the values of T_e/T_i increase, indicating stronger ion coupling, the screening of the potentials weakens.

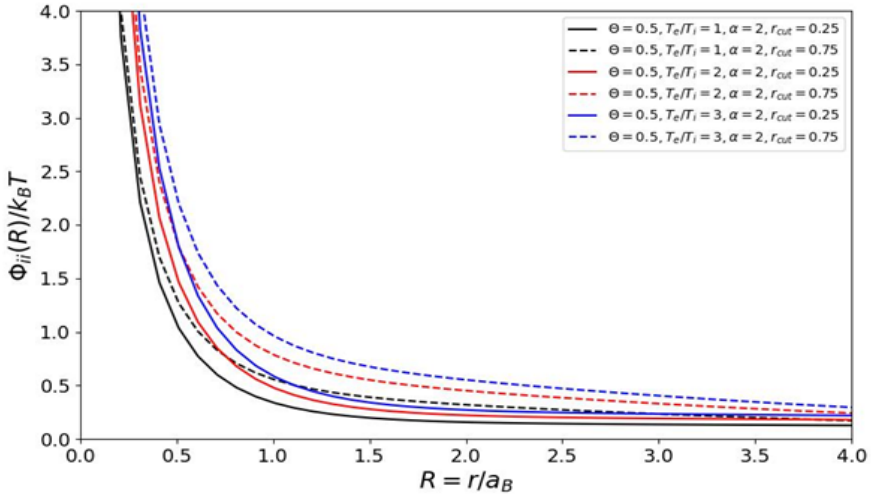

Figure 3 – The interaction potentials for i-i pairs at $\theta = 0.5$, $r_s = 1$ with α=2 for potential (1) for different values of $\frac{T_e}{T_i}$: $\frac{T_e}{T_i}$ =1 – black solid ($r_{cut} = 0.25$) and dashed ($r_{cut} = 0.75$) line, $\frac{T_e}{T_i}$ =2 – red solid ($r_{cut} = 0.25$) and dashed ($r_{cut} = 0.75$) line, $\frac{T_e}{T_i}$ =3 – blue solid ($r_{cut} = 0.25$) and dashed ($r_{cut} = 0.75$) line

Figures 4 and 5 show the radial distribution functions (RDFs) for i-i pairs at $r_s = 1$. In Figure 3 the results for potential (1) at $\theta = 1$ are depicted with varying values of Γ_i and r_{cut}. For $\Gamma_i = 1$ and $r_{cut} = 0.25$, the black solid line corresponds to α=2, while the dashed line represents α=6. For $\Gamma_i = 5$ with the same r_{cut}, the lines are shown in red. When $\Gamma_i = 10$ is considered, the green lines indicate the results for $r_{cut} = 0.25$ with the same line styles. Additionally, the blue lines show the screening potential (4), with solid lines for $\Gamma_i = 1$, dashed lines for $\Gamma_i = 5$, and dotted lines for $\Gamma_i = 10$.

In Figure 5 the RDFs for potential (1) at $\Gamma_i = 10$ and $\theta = 0.5$ are shown. Here, the black solid lines (α =2) represent $r_{cut} = 0.25$, while the dashed lines correspond to $r_{cut} = 0.75$. The red solid lines for $\theta = 1$ and $r_{cut} = 0.25$ are paired with dashed lines for $r_{cut} = 0.75$. The blue lines again depict the screening potential (4), with solid lines for $\theta = 0.5$ and dashed lines for $\theta = 1$.

In Figures 4 and 5 the radial distribution function (RDF) curves show how decreasing the r_{cut} strengthens the screening effects. The RDF for $r_{cut} = 0.25$ is positioned higher than that for $r_{cut} = 0.75$, indicating stronger attractive interactions between electrons and ions due to deeper negative minimum values of the non-screened electron-ion potential. Conversely, for fixed r_{cut}, increasing α shifts the potential minimum closer to the ion, making it steeper and resulting in a slightly higher RDF for α =6 compared to α =2. However, the difference between these RDFs is minor, while the distinction between potential (1) and the screening potential (4) is more pronounced, as the Yukawa model neglects the ion core effect, causing its RDFs (blue lines) to reach unity more quickly.

Because this is a non-isothermal plasma, RDF peaks increase with higher Γ_i values due to the difference between electron and ion temperatures, but overall curves with lower Γ_i values lie higher, as with the increasing coupling parameter, the probability of finding particles with the same charge (i.e., ions) decreases. And the difference in screening effects becomes more pronounced at lower θ values, indicating stronger coupling and strengthened electron-ion interactions.

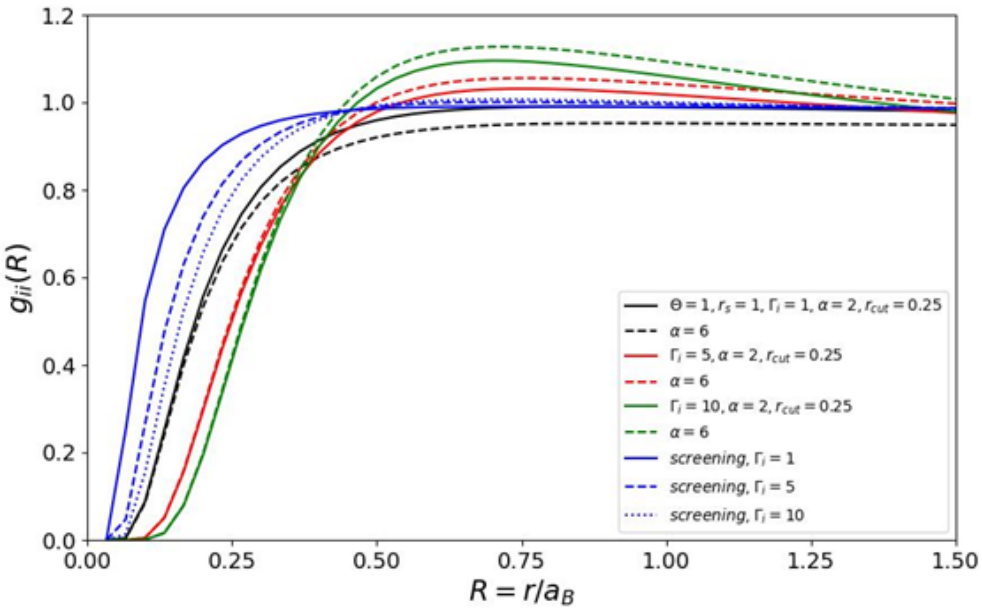

Figure 4 – The radial distribution functions for i-i pairs at $r_s = 1$ for potential (1) at $\theta = 1$ with $\Gamma_i = 1$, $r_{cut} = 0.25$ – black solid (α=2) and dashed (α=6) lines, $\Gamma_i = 5$, $r_{cut} = 0.25$ – red solid (α=2) and dashed (α=6) lines, $\Gamma_i = 10$, $r_{cut} = 0.25$ – green solid (α=2) and dashed (α=6) lines, blue lines – for screening potential (4) with solid ($\Gamma_i = 1$), dashed ($\Gamma_i = 5$) and dotted ($\Gamma_i = 10$)

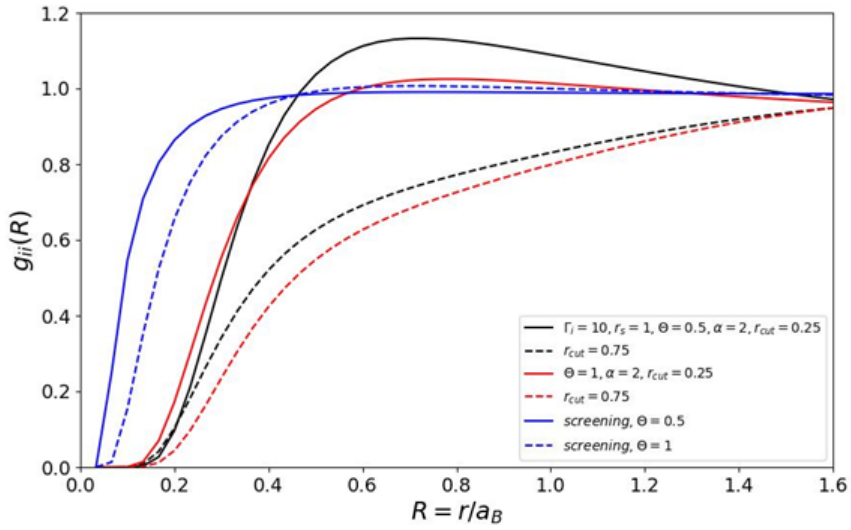

Figure 5 – The radial distribution functions for i-i pairs at $r_s = 1$ for potential (1) at $\Gamma_i = 10$ with $\theta = 0.5$, α=2 – black solid ($r_{cut} = 0.25$) and dashed ($r_{cut} = 0.75$) lines, $\theta = 1$, α=2 – red solid ($r_{cut} = 0.25$) and dashed ($r_{cut} = 0.75$) lines, blue lines – for screening potential (4) with solid ($\theta = 0.5$) and dashed ($\theta = 1$)

Figures 6 and 7 show correlation energy and equation of state (i.e., the ionic non-ideality corrections to the thermodynamic properties), respectively, calculated by solving equations (7–8) for the potential (1) and using potential (2) as micro potential $\varphi(r)$. The correlation energy and equation of state depend on the ratio of electron to ion temperatures, T_e/T_i, at a density parameter $r_s = 1$. Solid lines represent the case for $\theta = 1$, while dashed lines correspond to $\theta = 0.5$. The graphs include different values of α and r_{cut}: black lines indicate an interaction at $\alpha = 2$with $r_{cut} = 0.25$, while red lines represent the same $\alpha = 2$ but with $r_{cut} = 0.75$. Additionally, green lines show the impact of increasing the $\alpha = 6$ with a $r_{cut} = 0.25$, and blue lines show the $r_{cut} = 0.75$.

As Θ (and consequently temperature T) rises, the absolute values of non-ideality corrections decrease, showing a reduction in interactions within the system. The lower absolute values of the corrections to non-ideality are also observed for a larger cutoff radius of $r_{cut} = 0.75$ at a fixed α, as well as for a smaller $\alpha = 2$ at a fixed cutoff, due to a decrease in screening effects as the attraction between bound electrons and ions weakens. Conversely, as the values of Γ_i increase, signifying stronger coupling, the absolute values of the non-ideality corrections also rise.

Conclusions

In this study, we employed a novel ion-ion interaction potential that accounts for both screening from ionic cores and exchange-correlation interactions to analyze how the ion core effects impact the structural and thermodynamic properties of non-isothermal plasmas.

It should be noted that this study prioritizes investigating ion core effects in non-isothermal plasma over broad comparisons with other theoretical models or experimental data, as previous research has adequately addressed such comparisons [15, 16]. Our focus allows for a deeper exploration of ion-ion interactions without added complexity. While we did not include calculations with and without exchange-correlation interactions, prior work [15] has established that the differences in screening effects decrease at higher Θ, becoming negligible at $\Theta = 4$, which means in the regime of weakly or non-degenerate electrons, the effects of electronic exchange and correlation must be taken into account.

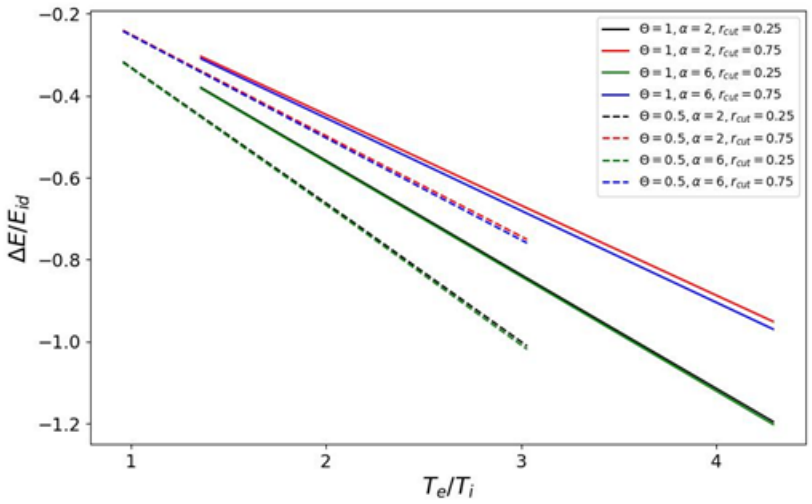

Figure 6 – The correlation energy for the potential (1) depending on relation between temperatures of electrons and ions $\frac{T_e}{T_i}$ using values of $\Gamma_i = 1, 5, 10$, at $r_s = 1$ for $\theta = 1$ ($T_e = 580\,000\ K$, solid lines) and $\theta = 0.5$ ($T_e = 290\,000\ K$, dashed lines): α=2, $r_{cut} = 0.25$ – black lines, α=2, $r_{cut} = 0.75$ – red lines, α=6, $r_{cut} = 0.25$ – green lines, α=6, $r_{cut} = 0.75$ – blue lines

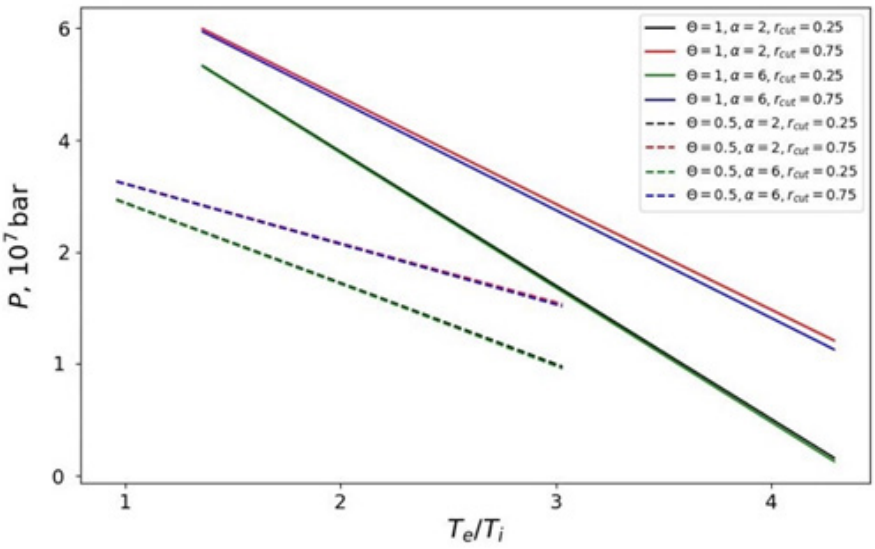

Figure 7 – The equation of state for the potential (1) depending on relation between temperatures of electrons and ions $\frac{T_e}{T_i}$ using values of $\Gamma_i = 1, 5, 10$, at $r_s = 1$ for $\theta = 1$ ($T_e = 580\,000\ K$, solid lines) and $\theta = 0.5$ ($T_e = 290\,000\ K$, dashed lines): α=2, $r_{cut} = 0.25$ – black lines, α=2, $r_{cut} = 0.75$ – red lines, α=6, $r_{cut} = 0.25$ – green lines, α=6, $r_{cut} = 0.75$ – blue lines

Our analysis demonstrates that as the distance between ions and electrons increases, the effective potential tends to converge towards a Yukawa-like screening potential. However, at shorter distances, the influence of strongly bound electrons creates a shielding effect that decreases the screening. The radial distribution functions (RDFs) further show the significance of adjusting parameters such as cutoff radius r_{cut} and core edge steepness α. For instance, a larger r_{cut} leads to a softer potential, while a smaller α results in a steeper potential at short distances.

Our analysis demonstrates that as the distance between ions and electrons increases, the effective potential tends to converge towards a Yukawa-like screening potential. However, at shorter distances, the influence of strongly bound electrons creates a shielding effect that decreases the screening. The radial distribution functions (RDFs) further show the significance of adjusting parameters such as cutoff radius r_{cut} and core edge steepness α. For instance, a larger r_{cut} leads to a softer potential, while a smaller α results in a steeper potential at short distances.

Additionally, we found that increasing Θ (and T), the absolute values of non-ideality corrections decrease, indicating fewer interactions in the system. The smaller absolute corrections to non-ideality are also seen with a larger cutoff radius of $r_{cut} = 0.75$ at a fixed α, as well as for a smaller $\alpha = 2$ at a fixed cutoff, due to reduced screening effects resulting from weaker attraction between bound electrons and ions weakens. On the other hand, as Γ_i increases (indicating stronger

Acknowledgments

This research has been funded by the Ministry of Science and Higher Education of the Republic of Kazakhstan (Grant No. AP19677200).

REFERENCES

1 Lifshitz, E.M., and Pitaevskii, L.P. Fizicheskaya Kinetika [Physical Kinetics] (Moscow: Physmathlit, 2002), pp. 96–97. (in Russian).

2 Ecker, G. Theory of Fully Ionized Plasmas (New York: Academic Press, 1972), pp. 132–134.

3 Ramazanov, T.S., Dzhumagulova, K.N., and Gabdullin, M.T. Effective Potentials for Ion-Ion and Charge-Atom Interactions of Dense Semiclassical Plasma. Physics of Plasmas, 17(4), 042703 (2010). https://doi.org/10.1063/1.3381078.

4 Ismagambetova, T.N., Moldabekov, Z.A., Amirov, S.M., et al. Dense Plasmas With Partially Degenerate Semiclassical Ions: Screening and Structural Properties. Japanese Journal of Applied Physics, 59, SHHA10 (2020). https://doi.org/10.35848/1347-4065/ab75b5.

5 Ramazanov, T.S., Dzhumagulova, K.N., and Moldabekov, Z.A. Generalized Pair Potential Between Charged Particles in Dense Semiclassical Plasma. Physical Sciences and Technology, 1(1), 48–54 (2018). https://doi.org/10.26577/phst-2014-1-114.

6 Ramazanov, T.S., Dzhumagulova, K.N., Gabdullin, M.T., Moldabekov, Z.A., and Ismagambetova, T.N. Development of Effective Potentials for Complex Plasmas. Physical Sciences and Technology, 6(3–4), 44–53 (2019). https://doi.org/10.26577/phst-2019-2-p6.

7 Ramazanov, T., and Moldabekov, Z. Dynamical collision frequency and conductivity of dense plasmas. Physical Sciences and Technology, 2(2), 53–57 (2016). https://doi.org/10.26577/2409-6121-2015-2-2-53-57.

8 Ramazanov, T.S., Kodanova, S.K., Issanova, M.K., Orazbayev, S.A., and Yelubaev, D.Ye. Temperature anisotropy relaxation processes in dense plasma. Recent Contributions to Physics, 75(4), 30–36 (2020). https://doi.org/10.26577/RCPh.2020.v75.i4.04

9 Pines, D., and Nozieres, P. The Theory of Quantum Liquids (New York: Benjamin, 1966), pp. 277–278.

10 Ashcroft, N.W., and Stroud, D. Theory of the Thermodynamics of Simple Liquid Metals. Solid State Physics, 33, 1–81 (1977). https://doi.org/10.1016/S0081-1947(08)60468-3.

11 Ashcroft, W., and Mermin, N.D. Solid State Physics (Philadelphia: Saunders College Publishing, 1976), p. 764.

12 Ramazanov, T.S., Kodanova, S.K., Nurusheva, M.M., Issanova, M.K. Ion core effect on scattering processes in dense plasmas. Phys. Plasmas, 28, 092702 (2021). https://doi.org/10.1063/5.0059297.

13 Ramazanov, T.S., Issanova, M.K., Aldakul, Y.K., Kodanova, S.K. Ion core effect on transport characteristics in warm dense matter. Phys. Plasmas, 29, 112706 (2022). https://doi.org/10.1063/5.0102528.

14 Ramazanov, T.S., Kodanova, S.K., Issanova, M.K., Kenzhegulov, B.Z. Influence of the ion core on relaxation processes in dense plasmas. Contrib. Plasma Phys. 64, e202300127 (2024). https://doi.org/10.1002/ctpp.202300127.

15 Ismagambetova, T.N., Muratov, M.M., Gabdullin, M.T., and Ramazanov, T.S. Influence of Ion Core on Structural and Thermodynamic Properties of Dense Plasma. Contributions to Plasma Physics, e70034 (2025). https://doi.org/10.1002/ctpp.70034.

16 Ismagambetova, T., Muratov, M., et al. The Influence of the Ionic Core on Structural and Thermodynamic Properties of Dense Plasmas. Plasma, 7(4), 858–866 (2024). https://doi.org/10.3390/plasma7040046.

17 Hansen, J.-P., McDonald, I.R. Theory of Simple Liquids (London, UK: Academic Press, 2000), pp. 100–102.

18 Gericke, D.O., Vorberger, J., et al. Screening of ionic cores in partially ionized plasmas within linear response. Phys. Rev. E, 81, 065401 (2010). https://doi.org/10.1103/PhysRevE.81.065401.

19 Moldabekov, Z.A., Dornheim, T. et al. Screening of a test charge in a free-electron gas at warm dense matter and dense non-ideal plasma conditions. Contrib. Plasma Phys., 62(2), e202000176 (2022). https://doi.org/10.1002/ctpp.202000176.

20 Moldabekov, Z.A., Groth, S., et al. Structural characteristics of strongly coupled ions in a dense quantum plasma. Phys Rev E, 98(2–1), 023207 (2018). https://doi.org/10.1103/PhysRevE.98.023207.

21 Groth, S., Dornheim, T., et al. Ab initio Exchange-Correlation Free Energy of the Uniform Electron Gas at Warm Dense Matter Conditions. Phys. Rev. Lett., 119, 135001 (2017). https://doi.org/10.1103/PhysRevLett.119.135001.

22 Bredow, R., Bornath, T., Kraeft, W.-D., and Redmer, R. Hypernetted Chain Calculations for Multi-Component and Non-Equilibrium Plasmas. Contributions to Plasma Physics, 53, 276–284 (2013). https://doi.org/10.1002/ctpp.201200117.

23 Kittel, C. Introduction to Solid State Physics, 8th Ed. (New York, USA: John Wiley and Sons, 2005), p. 696.

24 Springer, J.F., Pokrant, M.A., et al. Integral equation solutions for the classical electron gas. J. Chem. Phys., 58(11), 4863–4867 (1973). https://doi.org/10.1063/1.1679070.

25 Ng, K.-C. Hypernetted chain solutions for the classical one-component plasma up to Γ=7000. J. Chem. Phys., 61(7), 2680–2689 (1974). https://doi.org/10.1063/1.1682399.

26 Ramazanov, T.S., Ismagambetova, T.N., et al. The Influence of the Effects of the Bound Electrons on the Ion Structural and Thermodynamic Properties. IEEE Trans. Plasma Sci., 51(5), 1208–1211 (2023). https://doi.org/10.1109/TPS.2023.3267845.

27 Isihara, A. Statistical physics (New York, United States: Academic Press, 1971), p. 287.

[1,2,3]*Исмагамбетова Т.Н.,
PhD, сениор-лектор, ORCID ID: 0000-0003-4889-7526,
*e-mail: ismagambetova@physics.kz
[1,2,4]Муратов М.М.,
PhD, қауымдастырылған профессор, ORCID ID: 0000-0001-7270-9834,
e-mail: mukhit.muratov@gmail.com
[5]Усенов Е.А.,
PhD, қауымдастырылған физик-зерттеуші, ORCID ID: 0000-0001-7903-8674,
e-mail: yussenov@pppl.gov
[2,3,4]Габдуллин М.Т.,
PhD, ф.-м.ғ.к., профессор, ORCID ID: 0000-0003-4853-3642,
e-mail: gabdullin@physics.kz

[1]Ашық Түрдегі Ұлттық Нанотехнологиялық Зертхана (АТҰНЗ),
Әл-Фараби атындағы Қазақ ұлттық университеті, Алматы қ., Қазақстан
[2]Қолданбалы ғылымдар және ақпараттық технологиялар институты, Алматы қ., Қазақстан
[3]Қазақстан-Британ техникалық университеті, Алматы қ., Қазақстан
[4]Қазақстандық физикалық қоғам, Алматы қ., Қазақстан
[5]Принстон плазма физикасы зертханасы, Принстон, Нью-Джерси, АҚШ

ИОНДЫҚ НЕГІЗДІҢ ИЗОТЕРМИЯЛЫҚ ЕМЕС ПЛАЗМАНЫҢ ҚАСИЕТТЕРІНЕ ӘСЕРІ

Аңдатпа

Бұл жұмыста иондық негізден (қаңқа) де, алмасу-корреляциялық өзара әрекеттесуден де пайда болатын экрандалуды ескеретін иондық-иондық өзара әрекеттесудің жаңа потенциалын қолдану арқылы иондық негіздің изотермиялық емес плазмаға әсері зерттеледі. Нәтижелер қашықтықтың өсуімен тиімді потенциал Юкава түрінің экрандалу потенциалына жақындағанын көрсетеді, ал сонымен қатар одан да қысқа қа-

шықтықта электрондардың күшті байланысы экрандалуды әлсіретеді. r_{cut} кесу радиусының және α қаңқа жиегінің тік болуының әртүрлі мәндерінде потенциалдың және радиалды таралу функциялардың (РТФ) күй-өзгерісіне айтарлықтай әсер етеді. Байланыс параметрлерінің (Γ_i) жоғары мәндері электрон-иондық өзара әрекеттесуді күшейтеді, бұл өз алдына тереңірек потенциалды шұңқырларға және идеалдылыққа неғұрлым айқын түзетулерге әкеледі. Θ мәнінің өсуі идеалдылыққа түзетулердің абсолютті мәндерін азайтады, бұл жүйеде өзара әрекеттесудің мөлшерінің аздығын көрсетеді. Белілгенген бір α параметріндегі үлкен r_{cut} кесу радиусы әлсіз экрандалу әсеріне байланысты түзетулерді азайтады. Γ_i ұлғаюымен идеалдылыққа түзетулер байланыстың күшеюін көрсете отырып артады. Нәтижелер тығыз, изотермиялық емес плазманы зерттеу кезінде иондық негіздің әсерін есепке алудың маңыздылығын көрсетеді.

Тірек сөздер: тығыз плазма, иондық негіз, изотермиялық емес плазма, иондардың өзара әрекеттесу потенциалы, радиалды таралу функциялары,

[1,2,3]*Исмагамбетова Т.Н.,
PhD, сениор-лектор, ORCID ID: 0000-0003-4889-7526,
*e-mail: ismagambetova@physics.kz
[1,2,4]Муратов М.М.,
PhD, ассоциированный профессор, ORCID ID: 0000-0001-7270-9834,
e-mail: mukhit.muratov@gmail.com
[5]Усенов Е.А.,
PhD, ассоциированный физик-исследователь, ORCID ID: 0000-0001-7903-8674,
e-mail: yussenov@pppl.gov
[2,3,4]Габдуллин М.Т.,
PhD, к.ф.-м.н., профессор, ORCID ID: 0000-0003-4853-3642,
e-mail: gabdullin@physics.kz

[1]Национальная нанотехнологическая лаборатория открытого типа (ННЛОТ),
Казахский национальный университет им. аль-Фараби, г. Алматы, Казахстан
[2]Институт прикладных наук и информационных технологий, г. Алматы, Казахстан
[3]Казахстанско-Британский технический университет, г. Алматы, Казахстан
[4]Казахское физическое общество, г. Алматы, Казахстан
[5]Принстонская лаборатория физики плазмы, г. Принстон, Нью-Джерси, США

ВЛИЯНИЕ ИОННОГО ОСТОВА НА СВОЙСТВА НЕИЗОТЕРМИЧЕСКОЙ ПЛАЗМЫ

Аннотация

В данной работе изучается влияние ионного остова на неизотермическую плазму с использованием нового потенциала ион-ионного взаимодействия, учитывающего экранирующие эффекты как от ионного остова, так и от обменно-корреляционных взаимодействий. Результаты показывают, что с увеличением расстояния эффективный потенциал приближается к экранирующему потенциалу типа Юкавы, в то время как на более коротких расстояниях сильная связь электронов ослабляет экранирование. Различные значения радиуса обрезания r_{cut} и крутизны края остова α существенно влияют на поведение потенциала и радиальных функций распределения (РФР). Более высокие значения параметров связи (Γ_i) усиливают электрон-ионные взаимодействия, что приводит к более глубоким потенциальным ямам и более выраженным поправкам на неидеальность. Увеличение Θ уменьшает абсолютные значения поправок на неидеальность, что указывает на меньшее количество взаимодействий в системе. Больший радиус обрезания r_{cut} при фиксированном параметре α также уменьшает поправки из-за более слабого экранирующего эффекта. С увеличением Γ_i поправки на неидеальность возрастают, отражая усиление связи. Результаты показывают важность учета эффектов ионного остова при исследовании плотной неизотермической плазмы.

Ключевые слова: плотная плазма, ионный остов, неизотермическая плазма, потенциал взаимодействия ионов, радиальные функции распределения, термодинамические свойства.

Article submission date: 23.09.2025